CHAPTER 2

Theory and Methodology

2.1 General Theory

Seismic data processing helps image the subsurface using the seismic waves in which recorded at the surface. Migration techniques move the reflections to true subsurface positions, collapsing diffractions and increasing spatial resolution as we can see Figure 2.1. The migration algorithms are classified to three main categories: integral solution, finite-difference solution and frequency-wavenumber implementations (Yilmaz, 1987).

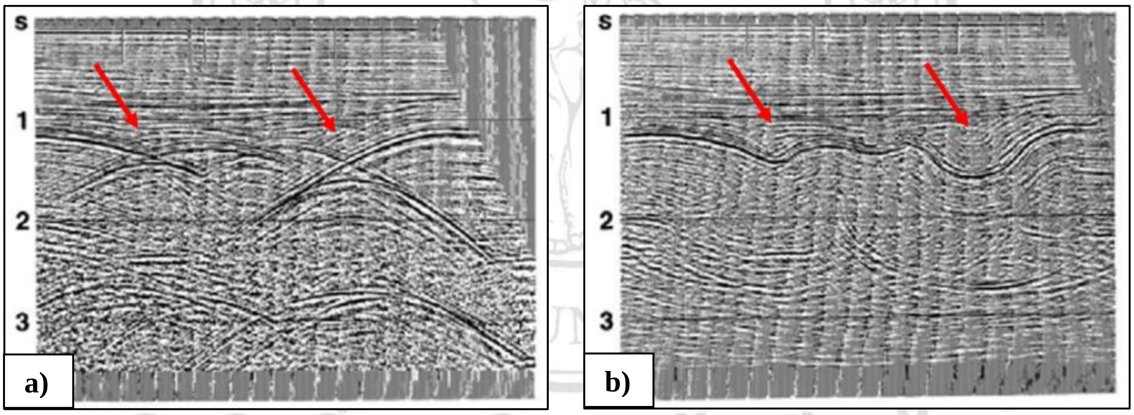

Figure 2.1 a) Unmigrated section and b) Migrated section (After Yilmaz, 1987).

After the migration process, the reflectors are steepened and shortened and only move in the up-dip direction (Yilmaz, 1987).

2.1.1 Zero-offset and Exploding reflector

When a stacked section is migrated, migration theory is suitable to record data with source and receiver at the same location (zero-offset, Figure 2.2). To develop a conceptual framework for discussing migration of zero-offset data, we have to examine two types of recording schemes: zero-offset and exploding reflector (Yilmaz, 1987).

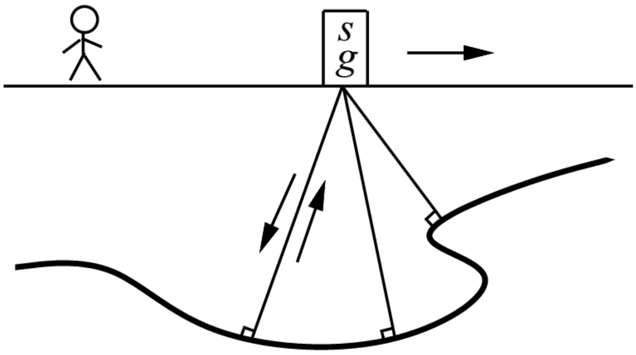

Figure 2.2 Zero-offset (Claerbout, 1985).

The zero-offset section (Yilmaz, 1987) is recorded by moving a single source and a single receiver along the line with no separation (Figure 2.2). The recorded energy follows ray-paths that are normal incidence to reflecting interfaces. Exploding reflectors (Yilmaz, 1987) are sources located along the reflecting interfaces (Figure 2.3). Consider one receiver located on the surface at each CMP location along the line. The sources explode in unison and send out waves which propagate upward. The waves are recorded by the receivers at the surface.

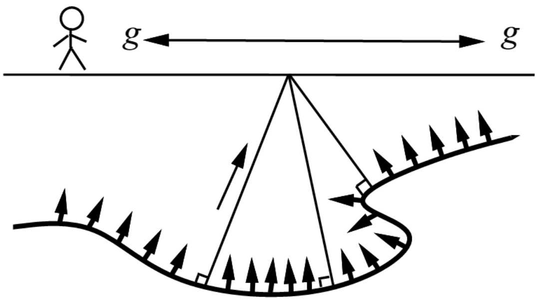

Figure 2.3 Exploding reflectors (Claerbout, 1985).

The resultant seismic section from the exploding reflectors model is largely equivalent to the zero-offset section, with one important difference. The zero-offset section is recorded as two-way travel-time (from source to reflection point to receiver), while the exploding reflectors model is recorded as one-way travel-time (from the reflection point at which the source is located to the receiver). To make the sections compatible, it is assumed that the velocity of the propagation is half the true medium velocity for the exploding reflectors model (Claerbout, 1985).

2.1.2 Downward continuation

Downward continuation (Claerbout, 2010) handles the multi-path that occurs in areas of complex geology, whereas Kirchhoff methods are far less reliable in complex velocity models (Gray et al., 2001). Downward continuation focuses on waves that propagate mainly in the vertical direction. For understanding downward continuation, the storm harbor experiment will be utilized (Figure 2.4) to describe the wavefield that propagates to subsurface then is recorded at the surface.

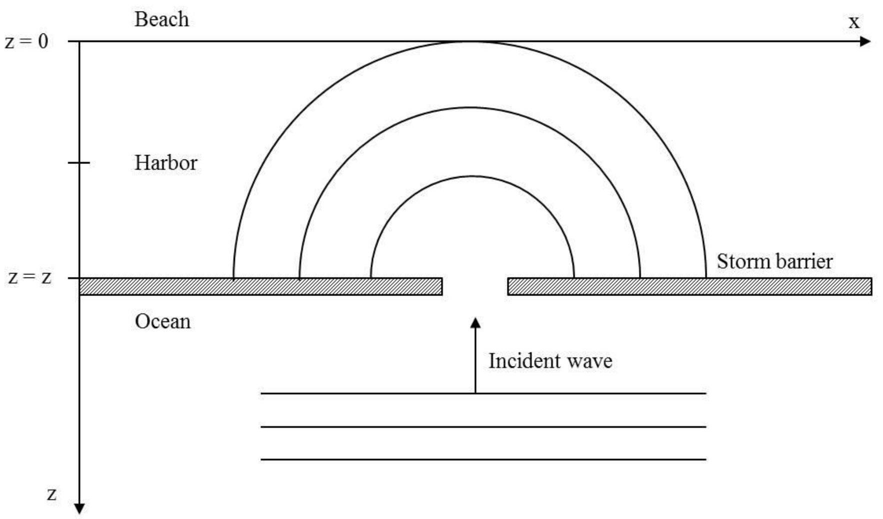

Figure 2.4 Storm barrier for understanding downward continuation (After Claerbout, 1985).

To extrapolate the wavefield recorded at surface to subsurface, the storm harbor experiment was introduced to explain the extrapolation of the wavefield from subsurface. Firstly, the upcoming wavefield which was recorded at surface *U(x,z=0,t)* where receivers located on the beach then move the receiver down to each depth. Finally, the receiver moves to the storm barrier the wavefield which is *U(x,z,t=0)* can then be obtained (Yilmaz, 1987).

2.1.3 Lateral Resolution

Lateral resolution is improved after migration by decreasing the Fresnel zone (Sheriff, 1980). The equation to calculate the radius of Fresnel zone is as follows:

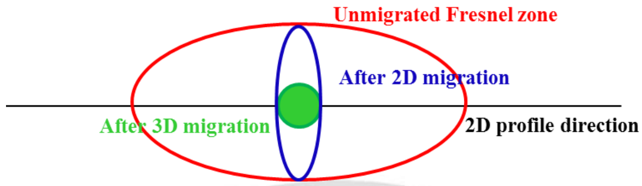

Figure 2.5 Fresnel zone.

The calculation of the radius of Fresnel zone (Figure 2.6) starts with equation 2.1.

$$(z+\frac{\lambda}{4})^2 = z^2 + R^2 \tag{2.1}$$

where z is depth, λ is wavelength and R is radius. So, we can find radius of Fresnel zone follow:

$$R=\left(\frac{\lambda\cdot z}{2}+\frac{\lambda^2}{16}\right)^{\frac{1}{2}} \approx \left(\frac{\lambda\cdot z}{2}\right)^{\frac{1}{2}} \tag{2.2}$$

Term of λ^2 will be small to be neglected. By using equation 2.3 and 2.4, equation 2.2 can be rewritten to equation 2.5 (Sheriff, 1980).

$$z=\frac{V\cdot t}{2} \tag{2.3}$$

$$V = f\cdot\lambda \tag{2.4}$$

$$R \approx \left(\frac{V}{2}\right)\cdot\left(\frac{t}{f}\right)^{\frac{1}{2}} \tag{2.5}$$

where V is velocity, f is frequency and t is time.

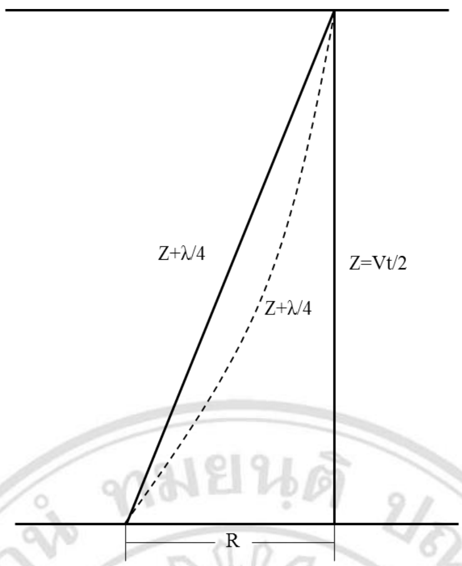

Figure 2.6 The geometry of Fresnel zone (After Sheriff, 1980).

2.1.4 Time and Depth Migration

Time migration creates a time section but it can be converted to depth by using the information of velocity and depth migration from a traveltime. The difference between time and depth migration are velocity. Time migration is looking for NMO and stack velocity which focuses the migrated image at each location. Thus, time migration performs constant velocity migration at each point. Depth migration uses interval velocity which similarly uses a model of subsurface. The interval velocities are averages of the subsurface velocities in which are over some characteristic distance. Therefore, the depth migration can model the seismic wavefield more accurately than time migration. Although depth migration cannot easily estimate velocity so geophysicists prefer time migration. The sections of time and depth migration were shown in Figure 2.7 (Gray et al., 2001).

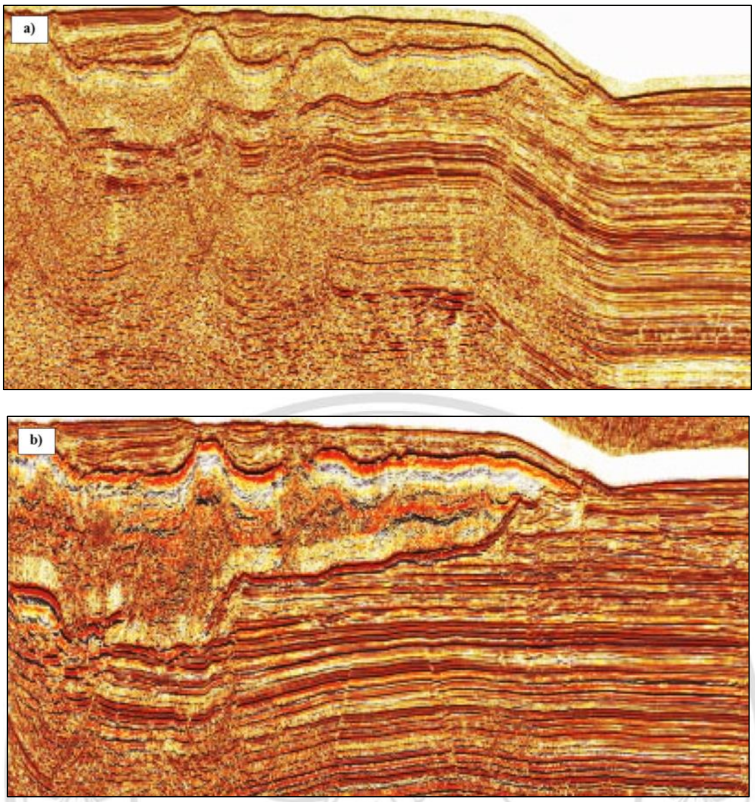

Figure 2.7 Migrated seismic section a) time migration and b) depth migration (Gray et al., 2001).

2.1.5 Wave Equation Migration

There are two main types of migration methods: ray-based and wave-based. Ray-based methods are Kirchhoff migration and Gaussian Beam migration that focus on computing travel-times by ray-tracing their summation. Wave-based methods are one-way and two-way wave equation migrations that focus on propagating the full measured wavefield. This thesis will focus on one-way wave equation, Gazdag and Finite-difference migration techniques.

2.1.6 Wavefield Extrapolation

The acoustic wave equation in 2-Dimensions describes a wavefield that propagates through the subsurface and is expressed as

$$\left(\frac{\partial^2}{\partial x^2}+\frac{\partial^2}{\partial z^2}-\frac{1}{v^2}\frac{\partial^2}{\partial t^2}\right)u(x,z,t)=0 \tag{2.6}$$

where *x* is the horizontal axis, *z* is the depth axis, *t* is time, and *v* is wave velocity. Wavefield recorded at the surface, *U(x, 0, t)*, is referred to as an upcoming wavefield. To determine the reflectivity of the subsurface *U(x, z, 0)*, the surface wavefield-upcoming wavefield *U(x, 0, t)* to depth *z* needs to be extrapolated. The process of obtaining the earth's reflectivity *U(x, z, 0)* from the observed wavefield *U(x, 0, t)* at the surface is called migration, and the reverse process is called modeling (Yilmaz, 1987). When equation 2.6 is Fourier transformed over *x* and *t* it gives equation 2.7:

$$k_z = \sqrt{\left(\frac{\omega}{v}\right)^2 - k_x^2} \tag{2.7}$$

where k_x is horizontal wavenumber, ω is temporal frequency, *v* is velocity and k_z is extrapolation wavenumber. One-way wave equation in the Cartesian coordinate system rewrite to equation 2.8:

$$u(z+\Delta z, k_x, \omega) = u(z, k_x, \omega)e^{(-ik_z\Delta z)} \tag{2.8}$$

2.1.7 Gazdag Migration

Gazdag migration method is based on wave equation migration that is applied phase-shifts in f-k domain. The Fourier transform can be used to obtain the wave equation which is downward continued to depth Δz by multiplying by filter operator (Claerbout, 2010).

$$e^{(-ik_z\Delta z)} \tag{2.9}$$

The acoustic wave equation is given by equation x using 2D-Fourier transform to obtain wave equation in frequency-wavenumber domain. For each frequency, equation 2.8 is employed to extrapolate the wavefield in frequency-wavenumber domain at depth *z* with phase-shift operator (equation 2.9) to obtain wavefield *U(k_x,z+*Δ*z,ω)* at depth *z*+Δ*z*. The previously step again repeated so that the inverse Fourier transform to space domain is then used to obtain the migration section at *U(x,z,t=0)* (Yilmaz, 1987). Gazdag migration method following these steps in Figure 2.8:

$$P(x,z=0,t)$$
$$\downarrow$$
$$2D\ Fourier\ transform$$
$$\downarrow$$
$$P(k_x,z=0,\omega) \longleftarrow exp(-ik_z z)$$
$$\downarrow$$
$$P(k_x,z,\omega)$$
$$\downarrow$$
$$\sum_{\omega} P(k_x,z=0,\omega)$$
$$\downarrow$$
$$1D\ Inverse\ Fourier\ transform$$
$$\downarrow$$
$$P(x,z,t=0)$$

Figure 2.8 Step of Gazdag migration method (After Yilmaz, 1987).

2.1.8 Finite-difference Migration

Finite-difference migration methods solve the wave equation based on the downward continuation scheme of the wavefield that propagated into subsurface and was then recorded at the surface. Yilmaz (1987) introduced the procedure to obtain the differential equation for Finite-difference migration. The acoustic wave equation (equation 2.6) and the Fourier transform of wavefield are used to obtain the dispersion relation (equation 2.7). They introduced the paraxial dispersion relation (equation 2.10) which is then approximated using Taylor expansion to find the dispersion equation for 15-degree Finite-difference time migration (equation 2.11).

$$k_z = \frac{2\cdot\omega}{v}\sqrt{1-\left(\frac{v\cdot k_x}{2\cdot\omega}\right)^2} \tag{2.10}$$

$$k_z = \frac{2\cdot\omega}{v}\left[1-\frac{1}{2}\left(\frac{v\cdot k_x}{2\cdot\omega}\right)^2\right] \tag{2.11}$$

Applying equation 2.11 into wave equation gives one-way wave equation (equation 2.12)

$$\frac{\partial}{\partial z}u(k_x,z,\omega) = -i\frac{2\cdot\omega}{v}\left[1-\frac{1}{2}\left(\frac{v\cdot k_x}{2\cdot\omega}\right)^2\right]u(k_x,z,\omega) \qquad (2.12)$$

After downward continuation steps, Yilmaz (1987) introduces the retard wavefield follow:

$$Q = P\cdot e^{-i\omega\tau} \qquad (2.13)$$

$$\tau = \int_0^z \frac{dz}{v(z)} \qquad (2.14)$$

where Q is retarded wavefield and τ and use equation 2.13 and 2.14 into equation 2.12. The 15-degree Finite-difference can be obtained from equation 2.15 and 2.16.

$$\frac{\partial^2 Q}{\partial z\partial t} = \frac{v}{4}\frac{\partial^2 Q}{\partial x^2} \qquad (2.15)$$

$$\frac{\partial Q}{\partial z} = 2\left[\frac{1}{v(z)} - \frac{1}{v(x,z)}\right]\frac{v}{4}\frac{\partial Q}{\partial t} \qquad (2.16)$$

The equation 2.15 is for collapse diffraction energy and equation 2.16 is thin-lens terms which are the terms of lateral variation. If the velocity are varies in lateral direction, this migration algorithm still includes thin-lens terms (this is depth migration), If the velocity only varies in vertical direction, the equation 2.16 will be a zero therefore the mean thin-lens terms will disappear. Only the diffraction terms will still be represented (this is the parabolic equation for time migration). Equation 2.15 can be rewritten into equation 2.17 (Yilmaz, 1987).

$$\frac{\partial^2 Q}{\partial \tau\partial t} = \frac{v^2}{8}\frac{\partial^2 Q}{\partial x^2} \qquad (2.17)$$

The dispersion relation was shown in Figure 2.9 relates to dispersion relation equation 2.10. The Finite-difference migration method based on 15 degree equation is used to allow the imaging of the 15 degree dipping reflector (Yilmaz, 1987).

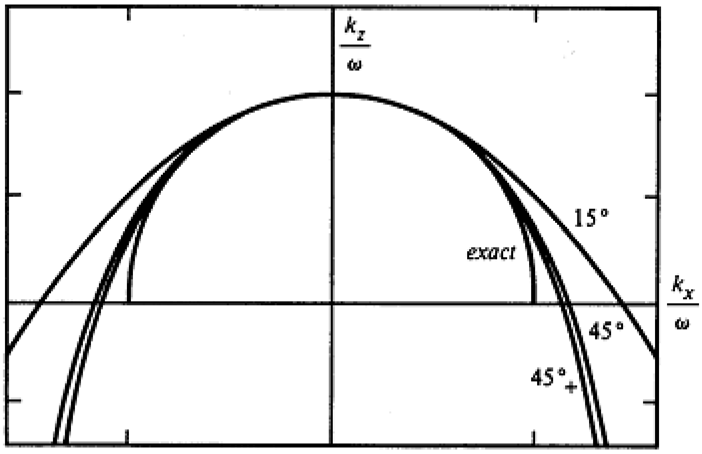

Figure 2.9 Dispersion relation (Claerbout, 2010).

2.2 Methodology

AWK software and Surfer software was utilized to prepare the velocity data, Matlab software to run migration then SeiSee software and Petrel software were used to show the results and obtain attributes (Figure 2.10).

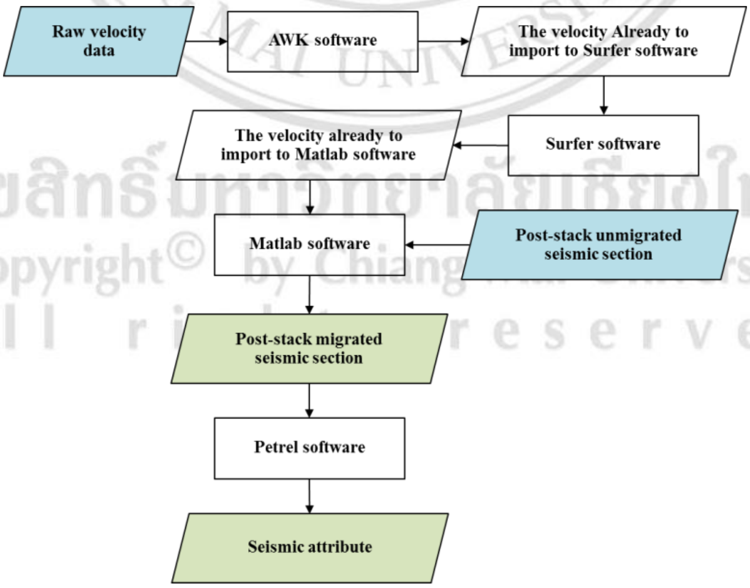

Figure 2.10 Workflow

2.2.1 Wavefield Extrapolation in log-polar Coordinates

The acoustic wave equation was introduced in equation 2.6. I will introduce transformation operator between log-polar and Cartesian coordinate systems as follows:

$$x = e^{p}\cos\theta \qquad z = e^{p}\sin\theta \tag{2.18}$$

where θ is propagation angle and p is extrapolation axis follow:

$$p = \log\sqrt{(x_l - x_i)^2 + (z_l - z_i)^2} \tag{2.19}$$

where x_l and z_l are origin location in log-polar coordinates x_i and z_i are the horizontal and vertical distances of each point from the origin in log-polar coordinates. The wavefield extrapolation equation in log-polar coordinate, which was solved by Naghadeh and Riahi (2013a) to show the relation between wave equation in Cartesian and log-polar coordinate systems

$$\frac{\partial u}{\partial p} = \frac{\partial u}{\partial x}\cdot\frac{\partial x}{\partial p} + \frac{\partial u}{\partial z}\cdot\frac{\partial z}{\partial p} = \frac{\partial u}{\partial x}\cdot e^{p}\cos\theta + \frac{\partial u}{\partial z}\cdot e^{p}\sin\theta \tag{2.20}$$

$$\frac{\partial u}{\partial \theta} = \frac{\partial u}{\partial x}\cdot\frac{\partial x}{\partial \theta} + \frac{\partial u}{\partial z}\cdot\frac{\partial z}{\partial \theta} = \frac{\partial u}{\partial x}\cdot e^{p}\sin\theta + \frac{\partial u}{\partial z}\cdot e^{p}\cos\theta \tag{2.21}$$

Equations 2.22, 2.23 and 2.24 can be used to solve equation 2.20 and 2.21.

$$\frac{\partial u}{\partial x} = \frac{\partial u}{\partial p}\cdot\frac{\partial p}{\partial x} + \frac{\partial u}{\partial \theta}\cdot\frac{\partial \theta}{\partial x} \tag{2.22}$$

$$\frac{\partial u}{\partial z} = \frac{\partial u}{\partial p}\cdot\frac{\partial p}{\partial z} + \frac{\partial u}{\partial \theta}\cdot\frac{\partial \theta}{\partial z} \tag{2.23}$$

$$\begin{bmatrix} \frac{\partial p}{\partial x} & \frac{\partial p}{\partial z} \\ \frac{\partial \theta}{\partial x} & \frac{\partial \theta}{\partial z} \end{bmatrix} = \begin{bmatrix} \frac{\partial x}{\partial p} & \frac{\partial z}{\partial \theta} \\ \frac{\partial z}{\partial p} & \frac{\partial z}{\partial \theta} \end{bmatrix}^{-1} = \begin{bmatrix} \frac{\cos\theta}{e^{p}} & \frac{\sin\theta}{e^{p}} \\ \frac{-\sin\theta}{e^{p}} & \frac{\cos\theta}{e^{p}} \end{bmatrix} \tag{2.24}$$

So, the second order derivation for log-polar coordinate systems was derived as follows:

$$\frac{\partial^2 u}{\partial p^2} = \frac{\partial}{\partial p} \cdot \left(\frac{\partial u}{\partial x} \cdot e^p \cos\theta + \frac{\partial u}{\partial z} \cdot e^p \sin\theta \right)$$

$$= \frac{\partial^2 u}{\partial x^2} \cdot \left(e^p \cdot \cos\theta\right)^2 + \frac{\partial^2 u}{\partial x \partial z} \cdot e^{2p} \cdot \cos\theta \cdot \sin\theta + \frac{\partial^2 u}{\partial z^2} \cdot \left(e^p \cdot \sin\theta\right)^2 + \frac{\partial^2 u}{\partial z \partial x} \cdot e^{2p} \cdot \sin\theta \cdot \cos\theta \qquad (2.25)$$

$$\frac{\partial^2 u}{\partial \theta^2} = \frac{\partial}{\partial \theta} \cdot \left(-\frac{\partial u}{\partial x} \cdot e^p \sin\theta + \frac{\partial u}{\partial z} \cdot e^p \cos\theta \right)$$

$$= \frac{\partial^2 u}{\partial x^2} \cdot \left(e^p \cdot \sin\theta\right)^2 - \frac{\partial^2 u}{\partial x \partial z} \cdot e^{2p} \cdot \sin\theta \cdot \cos\theta + \frac{\partial^2 u}{\partial z^2} \cdot \left(e^p \cdot \cos\theta\right)^2 - \frac{\partial^2 u}{\partial z \partial x} \cdot e^{2p} \cdot \cos\theta \cdot \sin\theta \qquad (2.26)$$

From equation 2.25 and 2.26, the wave equation in Cartesian can be rewritten to log-polar coordinate systems to equation 2.28.

$$\frac{\partial^2 u}{\partial \theta^2} + \frac{\partial^2 u}{\partial p^2} = \left(\frac{\partial^2 u}{\partial x^2} + \frac{\partial^2 u}{\partial z^2} \right) \cdot e^p \qquad (2.27)$$

$$\left(\frac{\partial^2}{\partial \theta^2} + \frac{\partial^2}{\partial p^2} - \frac{e^p}{v^2} \frac{\partial^2}{\partial t^2} \right) u(x, z, t) = 0 \qquad (2.28)$$

If equation 2.28 is Fourier transformed over θ and p, it gives:

$$k_p = \sqrt{\left(\frac{\omega \cdot e^p}{v} \right)^2 + \left(k_\theta\right)^2} \qquad (2.29)$$

Where k_p is wavenumber in log-polar coordinate, ω is temporal frequency and e_p/v is effective slowness. Then one-way wavefield extrapolation equation in log-polar coordinate system could then be obtained:

$$u(p + \Delta p, k_\theta, \omega) = u(p, k_\theta, \omega) e^{-i \cdot k_p \Delta p} \qquad (2.30)$$

2.2.2 Migration in log-polar Coordinate System

This migration aims to compare the results of migration between Cartesian and log-polar coordinate systems using post-stack unmigrated data. First, the Cartesian data is interpolated to log-polar coordinate. Then, interpolated dataset was migrated. Later, the migrated data was interpolated back to Cartesian coordinate and the results were compared (Figure 2.11).

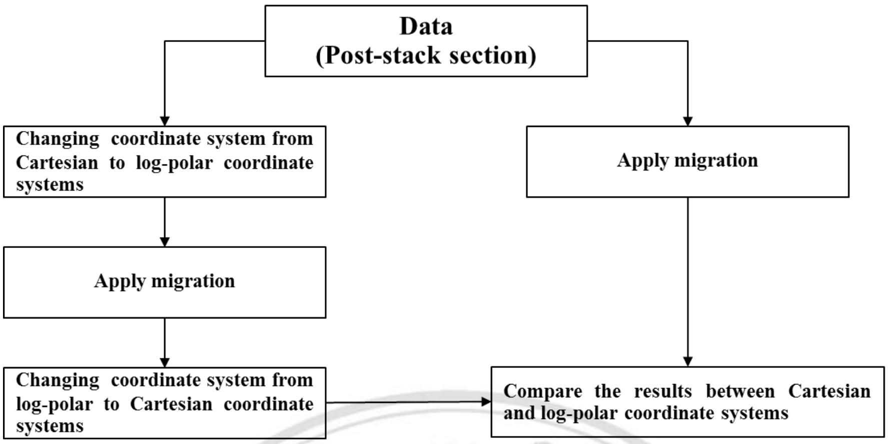

Figure 2.11 Proposed steps.

2.2.3 Database

The datasets are available from "The National Archive of Marine Seismic Surveys (NAMSS), a marine seismic reflection profile data archive consisting of data acquired by or contributed to the U.S. Department of the Interior agencies. The United States Geological Survey (USGS) is committed to safekeeping this data on behalf of the academic community and the nation. These data are provided for free and are open access (The United States Geological Survey, USGS)". The study areas are located in the region of Alaska, USA (Figure 2.12 and Table 2.1)

Table 2.1 The data from Alaska

Area	Survey	Line
Shelikof Strait, Alaska	W-26-80-WG	WSS140
Shelikof Strait, Alaska	W-26-80-WG	WSS160
Norton Sound, Alaska	W-21-80-BS	WNS324
Norton Sound, Alaska	W-21-80-BS	WSS325

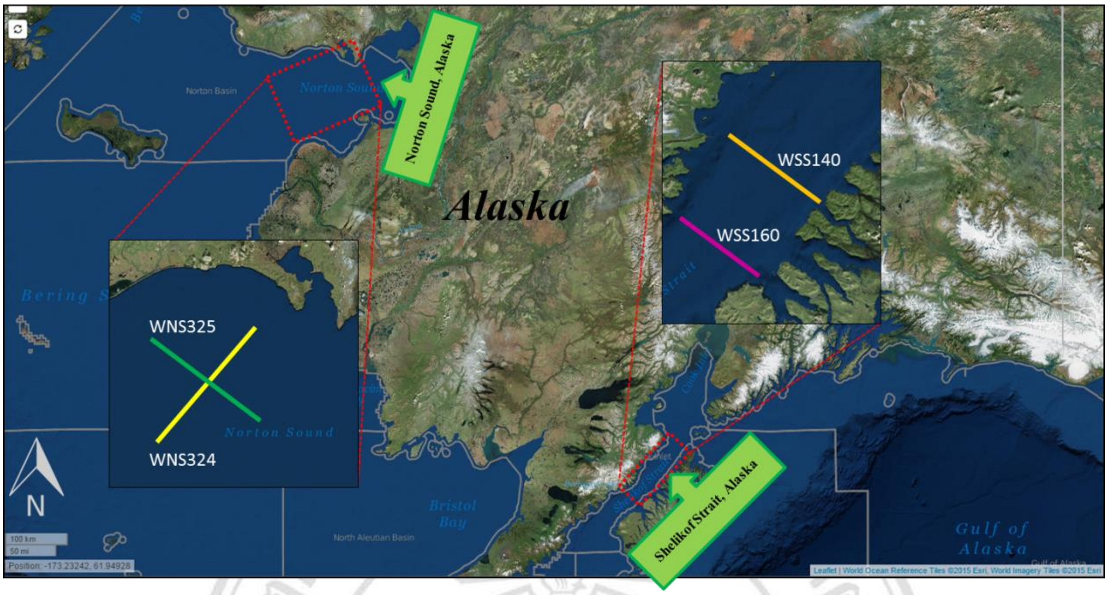

Figure 2.12 The study areas a) The data from Alaska and b) coastal of California (USGS, 2015).

2.2.4 Data Checking

Figure 2.13 highlights some bands of high amplitude in the stacked section which can cause problems with the data. These problem bands are not visible in Figure 2.14. So this stacked section was used for the post-stack migration.

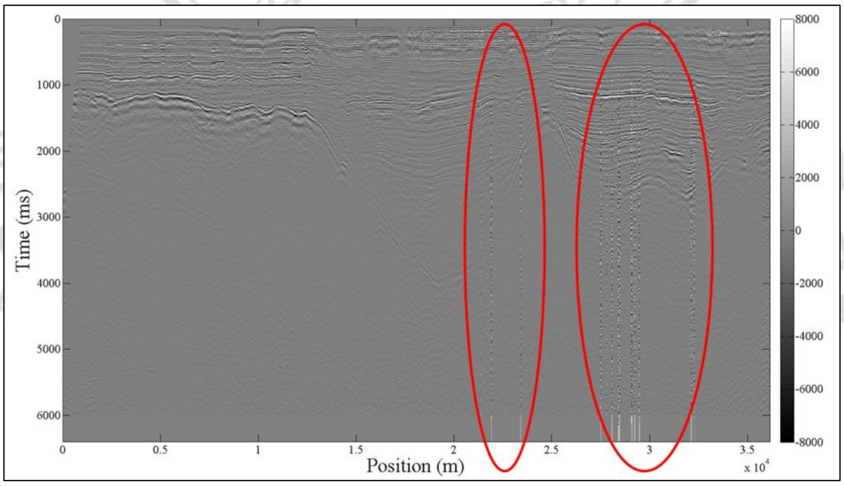

Figure 2.13 Post-stack data with the problem.

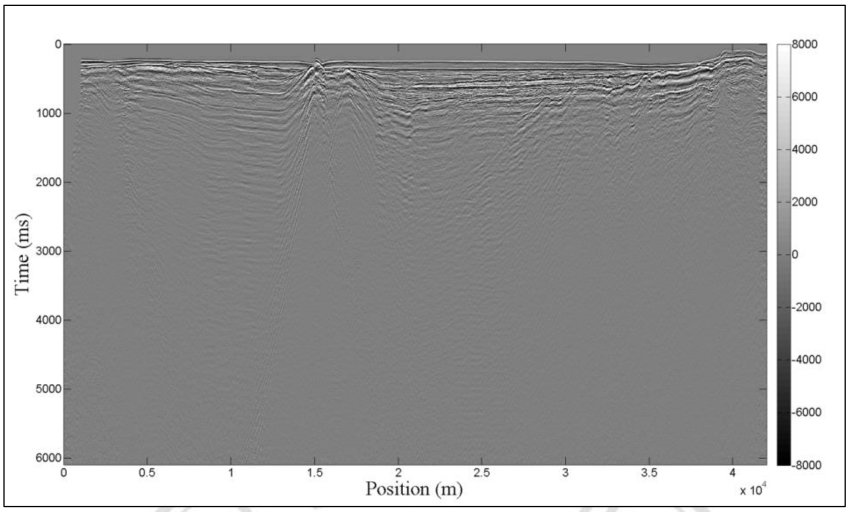

Figure 2.14 Post-stack data without the problem.

2.2.5 Preparing velocity

Velocity data was prepared to a format can be used for migration in the Matlab software. The AWK software and Surfer software are used to create the velocity data. The AWK software is language program designed to handle simple data (Close D. B., 1995).

```
CONT               WESTERN GEOPHYSICAL COMPANY
LINE       WNS-324
AREA       NORTON SOUND
INFO
COM1
COM2
PNMO
SPNT        96      97.          0          0
VELF        96       100 5000   800 6200 200010900 300012600 400013500
VELF        96      450013800 500014036 550014225 600014382
SPNT       168      169.         0          0
VELF       168       100 5000   700 5825   900 6525 200010600 300012400
VELF       168      400013300 450013626 500013882 550014088 600014257
SPNT       240      241.         0          0
VELF       240       100 5000   300 5350   700 6050 1000 6600 200010300
VELF       240      300012200 400013200 450013540 500013806 550014019
VELF       240      600014195
SPNT       312      313.         0          0
VELF       312       100 5000   500 5650   900 6000 1100 6425 1300 7400
VELF       312      2000 9700 300011800 400012900 450013280 500013577
VELF       312      550013815 600014010
SPNT       384      385.         0          0
VELF       384       100 5000   600 5925 1000 6075 1400 6800 1800 8100
VELF       384      2000 8700 300011200 400012400 450012850 500013199
VELF       384      550013478 600013705
SPNT       456      457.         0          0
VELF       456       100 5000   700 5875 1000 6075 1500 6900 1700 7600
VELF       456      1900 7950 300010900 400012200 450012679 500013049
VELF       456      550013344 600013585
SPNT       528      529.         0          0
VELF       528       100 5000   700 5875 1000 6050 1100 6275 1400 6675
VELF       528      1600 6925 2000 8400 300011000 400012300 450012764
VELF       528      500013124 550013411 600013645
SPNT       600      601.         0          0
VELF       600       100 5000   700 5950 1100 6225 1400 6600 1800 7375
```

a)

cdp	t	v
96	100	1524
96	800	1890
96	2000	3322
96	3000	3840
96	4000	4115
96	4500	4206
96	5000	4278
96	5500	4336
96	6000	4384
168	100	1524
168	700	1775
168	900	1989
168	2000	3231
168	3000	3780
168	4000	4054
168	4500	4153
168	5000	4231
168	5500	4294
168	6000	4346
240	100	1524
240	300	1631
240	700	1844
240	1000	2012
240	2000	3139
240	3000	3719
240	4000	4023
240	4500	4127
240	5000	4208
240	5500	4273
240	6000	4327
312	100	1524
312	500	1722

b)

Figure 2.15 The velocity data a) Before preparing and b) After AWK software (USGS, 2015).

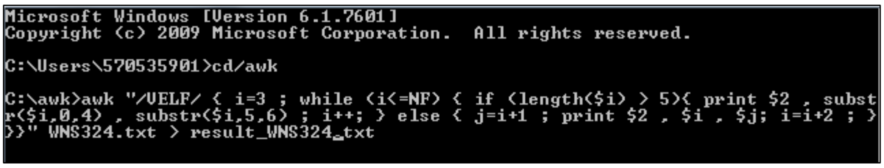

Figure 2.16 AKW code for preparing velocity data (Hutawarakorn, 2015).

After the velocity data was prepared with AWK software, the velocity section was created using with Surfer software. The velocity is known at some CDPs (Figure 2.17) so the known values are then interpolated across the whole section.

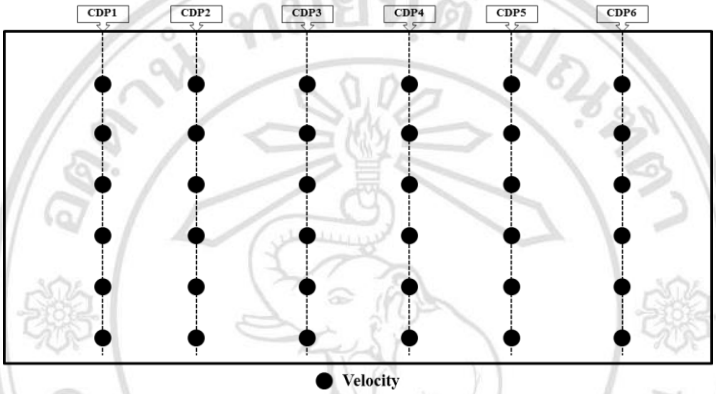

Figure 2.17 The example of velocity before interpolating.

By using Surfer software, the point of velocity for whole section can be interpolated (Figure 2.18).

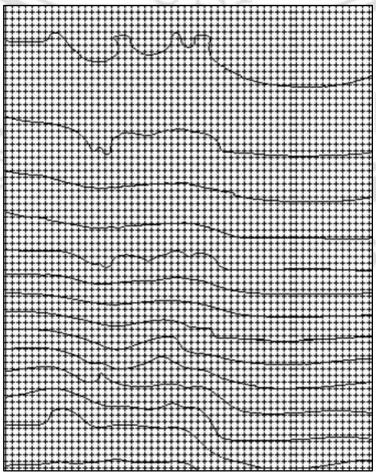

Figure 2.18 After interpolating velocity.

The interpolated velocity and post-stack unmigrated seismic section were then imported to Matlab software.

2.2.6 Changing coordinate system to log-polar coordinate system

The Cartesian velocity model and data were interpolated to the log-polar coordinate system for migration. The data were then interpolated back to the Cartesian coordinate system. This data were then compared to original Cartesian data as shown in Figures 2.19 to 2.21.

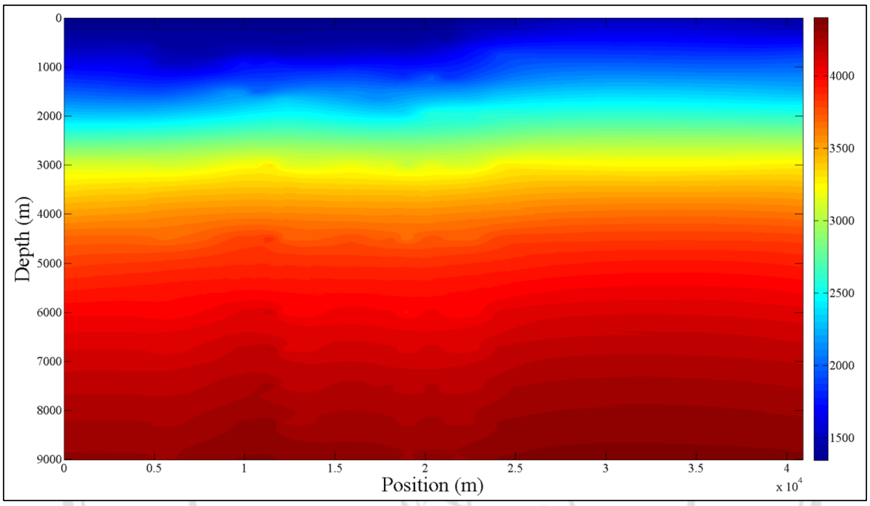

Figure 2.19 The velocity model before interpolated from Cartesian to log-polar coordinate.

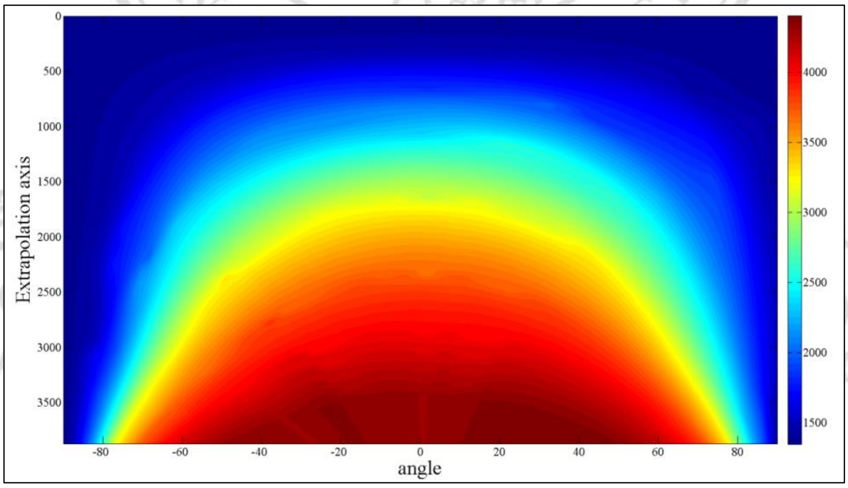

Figure 2.20 The effective slowness model in log-polar coordinate system.

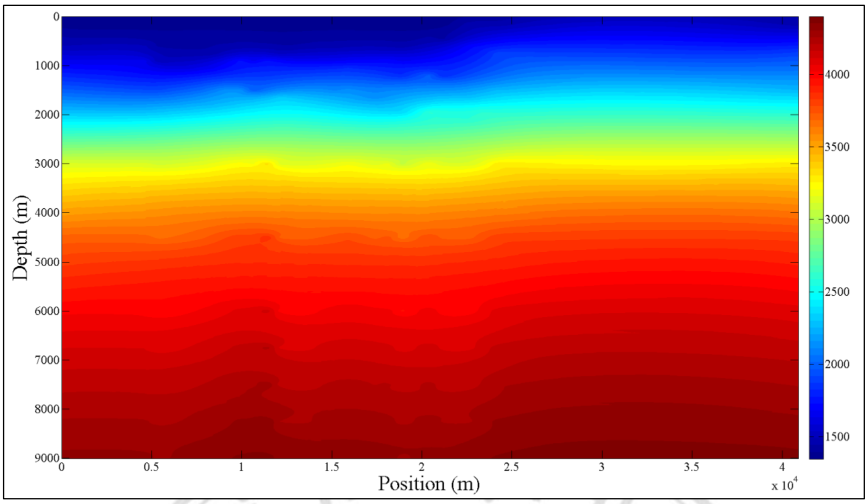

Figure 2.21 After interpolated back from Cartesian to log-polar coordinate systems.

The difference value between the section before interpolation of the data from Cartesian to LPCs and interpolated back to Cartesian coordinate system is mostly zero as highlighted in green on Figure 2.22.

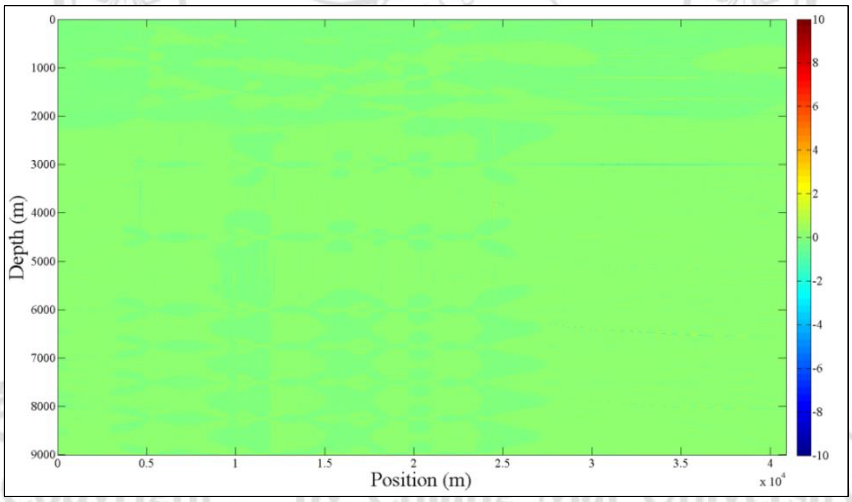

Figure 2.22 The difference value between the data before interpolated the data and interpolated back to Cartesian coordinate system.